

IAC-18,A6,3,5,x43898

## Measuring impact craters on the ISS Columbus Module

**Robin Putzar**Fraunhofer EMI, Germany, [robin.putzar@emi.fraunhofer.de](mailto:robin.putzar@emi.fraunhofer.de)**Max Gulde**Fraunhofer EMI, Germany, [max.gulde@emi.fraunhofer.de](mailto:max.gulde@emi.fraunhofer.de)**Dieter Sabath**Deutsches Zentrum für Luft- und Raumfahrt e.V. (DLR), Germany, [dieter.sabath@dlr.de](mailto:dieter.sabath@dlr.de)**Hauke Fiedler**Deutsches Zentrum für Luft- und Raumfahrt e.V. (DLR), Germany, [hauke.fiedler@dlr.de](mailto:hauke.fiedler@dlr.de)**Gerhard Drolshagen**Carl von Ossietzky Universität Oldenburg, Germany, [gerhard.drolshagen@uni-oldenburg.de](mailto:gerhard.drolshagen@uni-oldenburg.de)**Andy Braukhane**Deutsches Zentrum für Luft- und Raumfahrt e.V. (DLR), Germany, [andy.braukhane@dlr.de](mailto:andy.braukhane@dlr.de)**Andre Horstmann**TU Braunschweig, Germany, [andre.horstmann@tu-braunschweig.de](mailto:andre.horstmann@tu-braunschweig.de)**Carsten Wiedemann**TU Braunschweig, Institute of Space Systems, Germany, [c.wiedemann@tu-braunschweig.de](mailto:c.wiedemann@tu-braunschweig.de)**Martin Schimmerohn**Fraunhofer EMI, Germany, [martin.schimmerohn@emi.fraunhofer.de](mailto:martin.schimmerohn@emi.fraunhofer.de)**Frank Schäfer**Fraunhofer EMI, Germany, [frank.schaefer@emi.fraunhofer.de](mailto:frank.schaefer@emi.fraunhofer.de)

This is a slightly updated version of the publication (v1.1 as of 2018-09-25).

This paper presents the plan and first results of a photographic survey of the outer surface of the Columbus module with emphasis on the forward facing areas is proposed. This is to perform a status check of the Columbus meteoroid and debris protection system (MDPS) and to obtain information on the space debris and meteoroid environment of the ISS (International Space Station). The expected different impact crater count between zenith and forward facing panels will allow a distinction between man-made space debris and natural meteoroids. The majority of impacts is expected on the forward side of the cylindrical area. The survey is performed using image acquisition hardware available onboard the ISS. Different acquisition options are discussed, with the SSRMS (Canadarm2) tip LEE (Latching End Effector, i.e. the tip of the arm) camera being the most realistic option, but also the one with the lowest expected resolution. The predicted crater size distribution is calculated using ESA's MASTER model, and the proposed survey is compared with historical mission data that were used to validate the MASTER population in the past. The first part of the survey was performed on 5 September 2018, and some initial results are presented. The data acquired will be analyzed to yield size and position information of all craters identifiable from the video stream. The main aim of the survey is to generate measurement data for particle environment models (MASTER and ORDEM). This data will allow for a quantitative assessment of the particle impact risk for the entire ISS with an unprecedented accuracy. Also, it will allow to re-assess the validity of the impact risk assessments done for the Columbus module in the past. Since the Columbus module surface will be covered partially by the commercial platform "Bartolomeo" soon, there is a limited time slot for the actual performance of this study.

## I. INTRODUCTION

Impacts of fast traveling natural micrometeoroids and anthropogenic space debris are widely considered as the second major threat to humankind's presence in near-Earth space. The dimensions of particles that pose an impact threat to spacecraft range from micrometer-sized micrometeoroids to the 8-ton Envisat [1]. Larger objects are being tracked [2] and cataloged [3], so that collision avoidance maneuvers can be performed [4]. The size of objects in the NASA catalog ranges down to ten centimeters [5]. For impacts of smaller objects, collision avoidance maneuvers are not feasible since orbit parameters are generally not available. To cope with the hazard from such smaller sized particles, risk analyses are being performed routinely for spacecraft [6], which rely on particle environment models like MASTER and ORDEM [7]. The refinement and update of such models require impact flux data, which can be generated by in-situ detectors [8, 9], the analyses of retrieved hardware [10, 11] as well as radar and optical observation [12, 13]. Typical unmanned spacecraft structure walls can withstand particles up to about one millimeter in size [14], while the ballistic limit of manned modules is usually between one and two centimeters [15]. For unmanned spacecraft, impact consequences reach from component degradation [16] to mission loss [17, 18], which is generally associated with an economic risk [19]. For any manned missions, however, the particle environment poses a constant threat, which might inflict a loss of crew members or the entire crew. Therefore, generation of impact flux data is crucial not only to calculate and reduce the economic risk for unmanned

missions but also to reliably evaluate the risk for astronauts while in orbit.

### Available Validation Data

All small particle flux measurement methods are limited by the sensor area and the measurement duration, since the absolute particle flux decreases with increasing particle size, i.e. small particles are far more abundant than large particles. To obtain reliable data for particles larger than one millimeter, large sensor areas and long measurement durations are therefore necessary.

The MASTER population validation data for the small object regime currently relies on four returned surfaces from various space missions that are listed in Table 1 [12]. These are the LDEF experiment, the EuReCa mission and two Hubble service missions that replaced the solar arrays. The most important mission for the space debris population validation currently is the second Hubble service mission (3B) with an on-orbit duration of over 8 years and an area of almost 100 m<sup>2</sup> of which ca 40 m<sup>2</sup> were covered by solar cells [20].

### Objective

The primary goal of the activity described in this publication is to gain in-depth information on impacts of space debris and micro-meteoroids over the time period of the last 10 years in the ISS orbit. An emphasis lies on information about small particle fluxes which is sparsely available, since such long-term studies are seldom possible.

The results of this project will be compared to numerical model predictions and if required the models will be improved leading to more reliable impact risk assessments for future missions.

Mission	Deployment	Retrieval	On-orbit duration	Mean altitude	Area
LDEF	1984 April 06	1990 Jan 14	5a 9m 6d	475 km	39.13 m <sup>2</sup>
EuReCa	1992 Aug 01	1993 Jun 24	10m 23d	495 km	42.00 m <sup>2</sup>
HST-SA (SM1)	1990 Apr 24	1993 Dec 08	3a 7m 14d	614 km	81.00 m <sup>2</sup>
HST-SA (SM3B)	1993 Dec 04	2002 Mar 03	8a 2m 28d	614 km	97.00 m <sup>2</sup>

Table 1: Mission data of returned surfaces used for the MASTER population validation; based on table 3.18 from [12].

## SURVEY DESCRIPTION

A survey of a large ISS module, like Columbus, offers a unique opportunity to gain valuable new information on the abundant small size population of meteoroids and debris in space.

After 10 years in orbit in an altitude between 335 and 420 km the outside shell of the Columbus module offers an unprecedented source of information on space debris and micrometeoroid impacts in space. Hundreds of impact craters larger than 1 mm are expected, as presented in the "expected results" section below. The forward side of Columbus was nearly all the time facing

in flight direction, giving a reliable basis for comparison of the number of impacts with model predictions.

### Survey Location

The most interesting area for space debris impacts is the Columbus front side (rows 9-12, see red box in Fig. 1). Furthermore, the top side (row 1, see yellow line in Fig. 1) is valuable for reference impact data regarding micrometeoroids. The 3D-model in Fig. 2 underlines the high space debris impact risks particularly on the Columbus and ISS front areas.

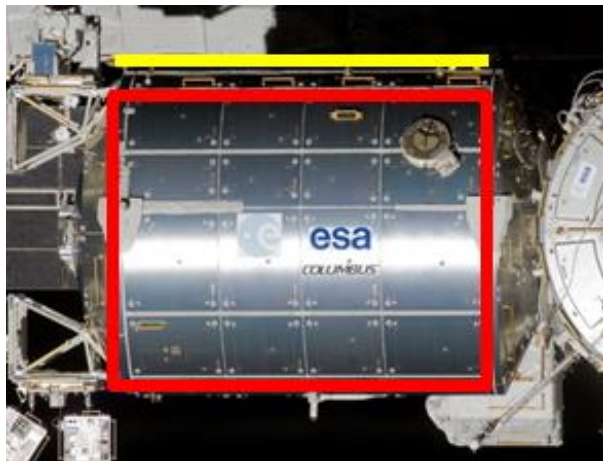


Fig. 1: Panel areas of interest (front presented by red box, top side by yellow line). Modified image from [21].

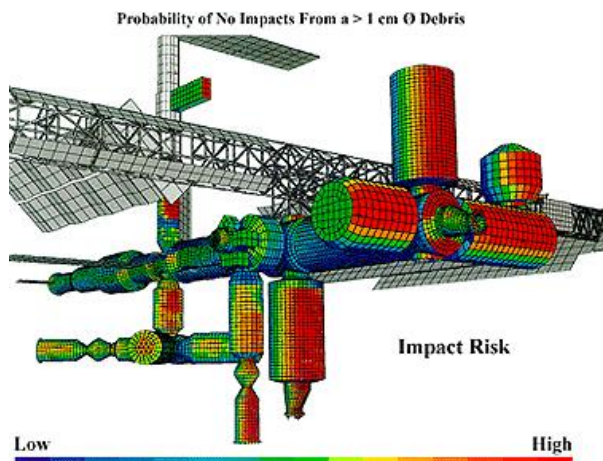


Fig. 2: Space debris impact risk on ISS modules for particles with a diameter of  $> 1$  cm. Image from [22].

#### Image Acquisition Opportunities at the ISS

For cost reason, only hardware that is available at the ISS is intended to be utilized for the optical survey. Available hardware currently comprises video cameras installed at the SSRMS (Canadarm2) and a DSLR (Nikon D4) carried along by astronauts during EVA activities. The prospective launch of VIPIR2 offers additional imaging capabilities.

Availability, expected image quality and resolution of the three options is discussed in the next three paragraphs.

##### SSRMS (Canadarm2)

Using the SSRMS (Space Station Remote Manipulator System) cameras, especially the tip LEE camera, the entire outer hull of the Columbus module is accessible. The SSRMS can be operated from ground, so no crew time is required for a scan. The SSRMS cameras output digital video data, which is downlinked to Earth. According to NASA ISAG, features down to 1 mm in

size can be detected from the video data, taking into account available camera resolution and safety distance regulations. Ref. [23] states 2 mm as available resolution. A possible issue is loss of feature data due to size or shadowing through video compression, cf. ref. [23].

##### EVA (Extra Vehicular Activity)

The Nikon D4 is used regularly by astronauts on EVA activities. A number of lenses are available on board of the ISS, with the following being used during EVA: 16 mm fish-eye, 28 mm, 35 mm and, 50 mm. The minimum focus distance of those lenses is between 250 and 500 mm. Using this camera (image resolution  $4928 \text{ px} \times 3280 \text{ px}$ , sensor size  $36 \text{ mm} \times 24 \text{ mm}$ ) and the 28 mm lens at 500 mm object distance, the per-pixel resolution is 0.12 mm, and the field of view is  $0.6 \text{ m} \times 0.4 \text{ m}$ . With a longer focal length lens, both the per-pixel resolution and the field of view decrease. While the theoretical resolution of pictures taken during an EVA is greater than pictures from SSRMS, a number of drawbacks are associated with this method. The most important is that EVA time is required for this imagery, which is sparsely available and extremely expensive. A second important drawback is that it is not easy for astronauts to create high-quality images during EVA, especially at such short distances. According to NASA astronaut trainers, this is mainly due to camera handling issues, which is difficult while in an EVA suit. Therefore, the theoretical resolution cannot be guaranteed to be achieved.

##### VIPIR2

Finally, the NASA ISAG team has pointed to the possibility of using VIPIR2 (Visual Inspection Poseable Invertebrate Robot 2) to obtain optical images with higher resolution. VIPIR2 is scheduled for launch to ISS during Robotic Refueling Mission 3 in 2018. VIPIR2, like VIPIR, will be operated as “tool” using SSRMS. Like SSRMS, VIPIR2 can be operated from ground with no crew time being required. The available resolution of VIPIR2 will depend on the minimum object distance, i.e. the minimum allowed operation distance from Columbus. The expected resolution will be 0.013 mm/px at 60 mm (2.5 in) distance, or 0.05 mm/px at 180 mm (7 in) distance. Such short distances are well inside the 2 ft clearance zone that is usually respected during SSRMS operation. Therefore, such a short distance scan would require special approval, which would require a strong reason to be performed.

In summary, utilization of the SSRMS cameras is the most cost-effective solution to obtain images from the Columbus outer hull. The major disadvantage of SSRMS images is the comparatively small resolution of down to 1 mm.

Because EVA/DSLR images are expensive and the theoretical resolution cannot be guaranteed, this option is considered only as potential piggy-back activity if an EVA is already planned close to the Columbus module.

Utilization of VIPIR2 would enable higher resolution images with similar advantages as SSRMS images, presumably at somewhat higher costs, and intruding into the 2 ft zone. It should be noted that VIPIR2 is not yet on-board ISS, and that it is not yet decided how long VIPIR2 will stay in orbit. Therefore, availability of VIPIR2 for this survey was an open issue.

### Expected Results

By evaluating the mission profile for the ISS and the Columbus front surface with ESA's MASTER-2009 space debris model, the expected flux and number of impacts can be assessed. With more than 10 years in operation, the impact data of space debris on the Columbus front side will give valuable statistical information on the space debris environment. The expected number of crater diameters ( $d_c$ ) larger than 1 mm can be derived from the corresponding flux analysis which is shown in Fig. 3 (dark blue line). For the conversion of particle fluxes to crater diameters, the equation from McDonnell and Sullivan was used, which is equation (6.5) in ref. [24]. For crater diameters larger than 1 mm, the expected flux corresponds to approx.  $32 / (\text{m}^2 \cdot \text{a})$ , which gives the number of expected impacts  $N(d_c)$  per area

$$N(d_c > 1 \text{ mm}) \approx 32 \frac{\text{Impacts}}{\text{m}^2 \text{a}} \cdot 10 \text{ a} = 320 \frac{\text{Impacts}}{\text{m}^2}$$

This gives a first approximation for the expected number of observed impacts. The number of expected impact per area for larger diameter thresholds can be found in Table 2.

$d_c$	$N$	$d_c$	$N$
> 1 mm	$\approx 320 / \text{m}^2$	> 6 mm	$\approx 2 / \text{m}^2$
> 2 mm	$\approx 100 / \text{m}^2$	> 7 mm	$\approx 0.6 / \text{m}^2$
> 3 mm	$\approx 36 / \text{m}^2$	> 8 mm	$\approx 0.23 / \text{m}^2$
> 4 mm	$\approx 10 / \text{m}^2$	> 9 mm	$\approx 0.01 / \text{m}^2$
> 5 mm	$\approx 4 / \text{m}^2$	> 10 mm	$\approx 0.01 / \text{m}^2$

Table 2: Number of expected impacts  $N$  per  $\text{m}^2$  after 10 years of exposure on the front face of Columbus over different conchoidal fracture diameter thresholds  $d_c$ .

The MASTER-2009 population is validated up to 1 May 2009. The validation is based on the most recent measurement data available at that time (radar and optical observations), cf. chapter 3.4 in ref. [12]. The remaining part of the evaluation is done by using a future projection of the environment. During the currently ongoing activity to update the MASTER population, the number of on-orbit debris tend to increase. Therefore, it is expected that the observed number of impacts for the Columbus front side will be slightly higher than

currently assessed. It is important to know that the diameter spectrum shows the number of impact for different crater diameters. Using damage equations, which are very well defined for aluminum targets, the impacting object true diameter can be assessed. This is visualized by the light blue line in Fig. 3. For conchoidal diameters larger than 1 mm in diameter, the corresponding minimum true object diameter can be estimated to approximately  $85 \mu\text{m}$ .

The relative contribution of meteoroids and space debris will depend on the orientation of the target area. For a front facing Columbus surface the flux share for conchoidal fracture diameters larger than 1 mm are approximately 38 % meteoroids and 62 % artificial debris (based on predictions by MASTER). This is shown in Fig. 4. For space facing surfaces, the majority of impacts will come from meteoroids. For a distinction of meteoroid and debris fluxes, it is therefore important to survey surfaces with different flight orientation and, most important, front and zenith facing areas.

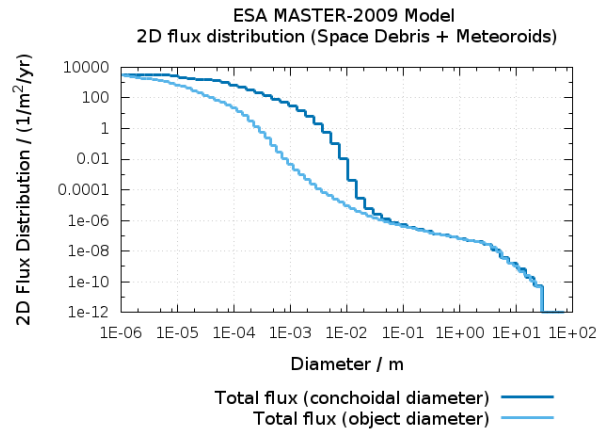


Fig. 3: Cumulative flux distribution as function of the diameter for the front surface of the Columbus module.

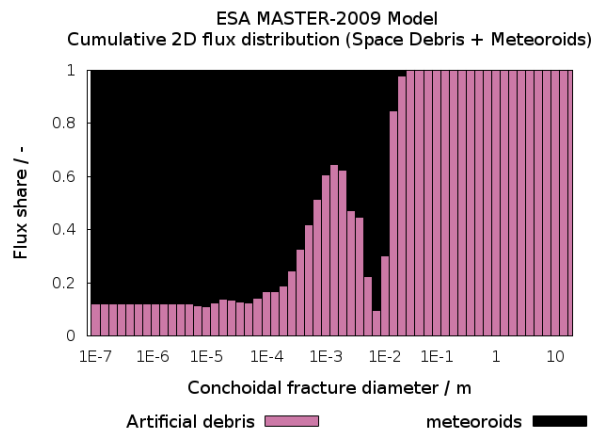


Fig. 4: Flux share as function of the conchoidal fracture diameter for the front surface of the Columbus module.



### Surface Size for Survey

In general, the maximum amount of information will be gained by a survey of the largest possible surface area and of outer surfaces pointing at different directions. However, valuable information can be obtained already if a limited area of a few m<sup>2</sup> is imaged.

The expected high impact flux for smaller particles motivates a two-step approach for the survey, in which a large surface is scanned with somewhat reduced resolution (e. g. 3–4 mm upward), and a smaller part of the surface with the highest possible resolution.

### Conduction of Survey

Together with NASA Robotics Operation, the requirements for the survey have been discussed, and the following requirements were defined:

- SSRMS Tip LEE Camera will be used for each survey, which will be executed by means of FOR OCAS
- Tip LEE Camera focal length set to 75 mm (HFOV 6.6 °)
- Angle of Incidence: less than 45 ° (from the surface normal) is acceptable but less than 30 ° is desired
- 10 % overlap of survey passes (to ensure full coverage and make stitching together of images easier)
- Maximum rate of translation: 1.5 meter/min
- SSRMS will remain outside of 2 ft clearance zone to all structure throughout the surveys

The scan was divided into two sections, each of which can be executed on the same day or on different days as required:

- Section A: survey Columbus panel row 1 (zenith-facing)
  - Survey all of Columbus panel row 1 with the Tip LEE as close to 5 ft away from Columbus surface as feasible given proximity constraints.
  - Survey one panel in Columbus Panel Row 1 with the Tip LEE as close to 2 ft away from Columbus surface as feasible given proximity constraints.
- Section B: survey Columbus panel rows 9–12 (nearly ram-facing)
  - Survey all of Columbus panel rows 9–12 with the Tip LEE as close to 5 ft away from Columbus surface as feasible given proximity constraints.
  - Survey one panel in Columbus panel row 10 with the Tip LEE as close to 2 ft away from Columbus surface as feasible given proximity constraints.

Further design of the SSRMS trajectories by Kenton Kirkpatrick from NASA Robotics Operations Branch assured that the survey can be performed pretty close to

orthogonal in almost all of the survey passes, and the entire survey is within the desired incidence angle of 30 °.

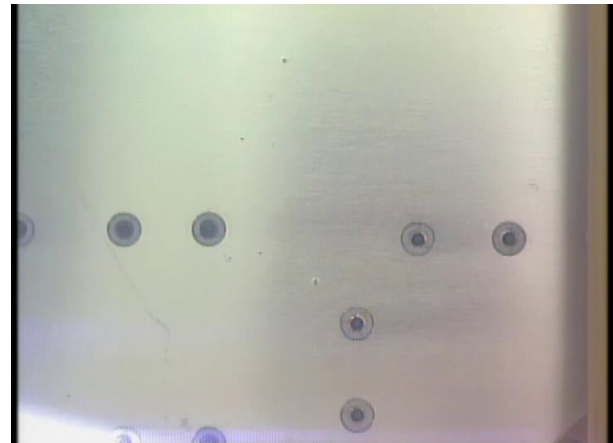


Fig. 5: Sample video frames from the survey. Time indices and panel numbers (from top to bottom): 2018 GMT 248 22:15 COL/02-01, GMT 249 00:07 COL/03-01, GMT 249 00:20 COL/03-01. Image credit ESA / NASA.

For distances to the module on the 5 ft surveys, variations in obstacles drive the LEE distance to the panels to vary between 5 ft and 7 ft away. But in all cases, the distance to the module panels is constant throughout a particular imagery pass. In most cases, the SSRMS LEE distance to the panel is around 65 in.

For the close-up inspections, panel 03-01 was chosen for the zenith side (section A) and panel 02-10 for the ram side (section B). This was because they have the fewest objects in the way, allowing for the SSRMS to be closer to the panel during the inspection. Throughout these two close-up inspections, the SSRMS LEE distance to the panel is around 27 in.

On 5 September 2018, section A of this survey was conducted successfully. Fig. 5 shows some sample video frames from this survey. A reliable scale is not yet available at this stage of the analyses. The top image is from the 5 ft scan, the two bottom images are from the 2 ft scan. Section B of this survey was performed between 21 and 23 September 2018.

The time frame for this survey was limited by the installation of the CoKa terminal and Bartolomeo, both scheduled for 2019. Also the availability of SSRMS for such a survey is limited by other operational considerations.

### IMAGE PROCESSING

Image post-processing will be performed on ground. Using suitable algorithms, crater data will be extracted using automatic or semi-automatic algorithms as exemplary described in the following. Fraunhofer EMI has performed similar analysis on witness plates, cf. [25]. The output will be a list that contains crater position and size. This list is then available for further analysis and can also be shared with NASA and other agencies for further model validation.

The general methodology of the crater extraction algorithm can be roughly divided in three parts: for each region of interest within a respective part of a video frame, we (1) remove the background gradient stemming from inhomogeneous lighting and material conditions, (2) perform a binarization of the image for crater identification and localization and (3) use the extracted crater position for the original image to determine the crater size and other characteristics such as its ellipticity.

First, we choose a suitable size for the region of interest with a video frame or composite image stitched from multiple such frames. Fig. 6 displays an exemplary region extracted from the center of the middle video frame shown in Fig. 5. Here, we converted the image to a grey scale matrix to enhance contrast with respect to the original, colored image.

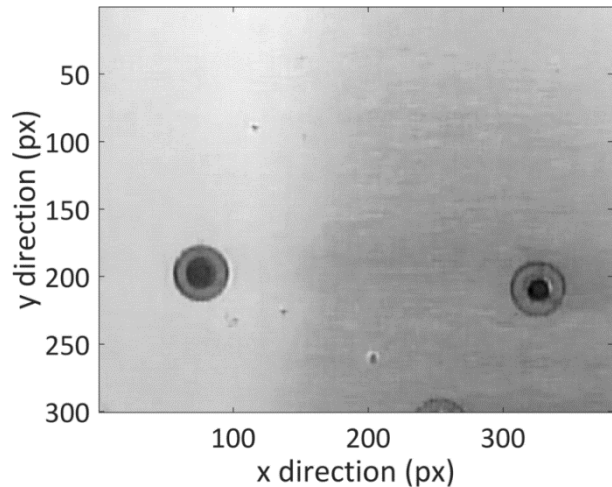


Fig. 6 Area of interest extracted from center frame of Fig. 5 with few craters. Strong lighting gradient visible.

At this state, due to inhomogeneous lighting conditions, the craters are difficult to extract for an automated image-processing algorithm: Craters in areas with higher grey values (i.e. more light) seem more pronounced than those in darker regions. We apply two-dimensional Fast Fourier Transformation to efficiently remove the slowly changing image background brightness variations (Fig. 7). This offers the additional benefit of an enhanced contrast, which improves the applicability of the next step: image binarization.

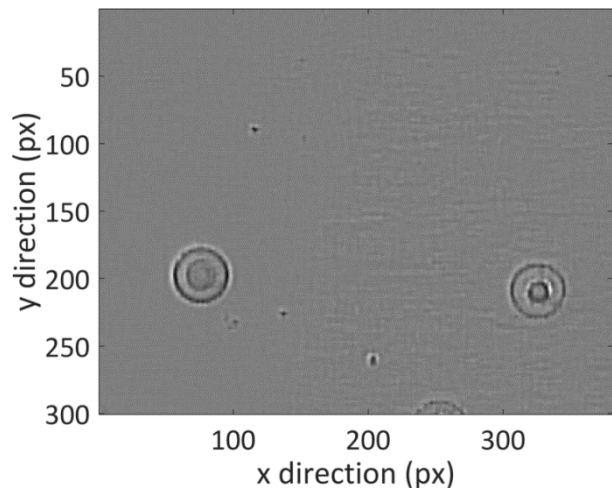


Fig. 7 Area of interest with lighting gradient removed.

The idea is to optimally separate the foreground information, i.e. craters, screws and other features on the hull, from the relatively noisy background. Specifically, we apply Otsu's method assuming such a bi-modal histogram [26]. Fig. 8 displays the resulting binary. An algorithm can now easily find the crater positions, indicated by the orange (small) and red (larger) circles. Moreover, an automatic differentiation between craters

and other features such as screws and scratches on the spacecraft hull can be implemented using a flood-fill or similar algorithm and perform a shape-analysis of the resulting areas.

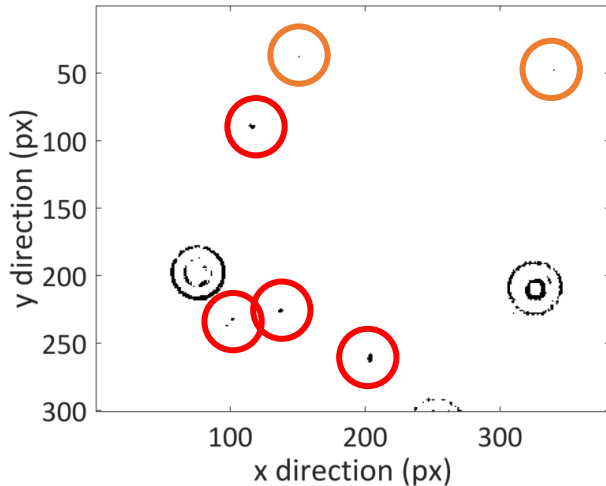


Fig. 8 Binarized image with indicated crater positions: Very small craters (orange circles), larger craters (red circles).

Subsequently, we employ the extracted crater positions in the original image to determine the crater size along different axis. Fig. 9 displays the inverted image cross-sections through one such crater along the x (blue) and y (red) directions with respect to the video frame coordinate system. The solid lines display the change in brightness and the dashed lines a respective Gaussian fit. For craters of a few pixels size, a comparison of the crater size in different directions can determine the degree of ellipticity and help infer on the potential impact direction.

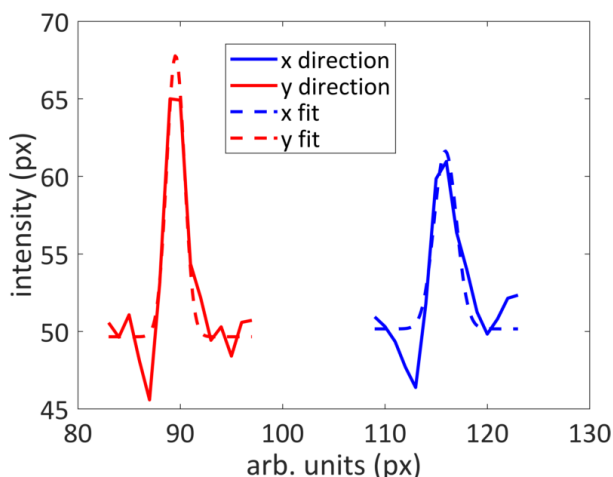


Fig. 9 Extracted crater size in x (blue) and y (red) direction (solid lines) with respective fits (dashed lines).

Notably, in the future analysis of the data, we will employ physical units to describe the crater characteristics. Moreover, all computational steps will be performed in the same coordinate system.

## DISCUSSION

As of writing of this publication, only the first part of the survey has been performed. The video data has only recently arrived at the team. Therefore, no thorough analysis could be performed so far. However, a first survey of the video data showed that there are many visible features on the zenith panels. Most of the features are craters, some may be holes, which is to be confirmed by further analyses.

### Expected Impact

The raw data from this survey will provide a status overview of the Columbus module meteoroid and debris protection system. The processed data, which will be available after completion of the image analyses, are the basis for further assessments, particularly the re-evaluation of the validity of the impact risk assessments done for the Columbus module in the past, and an update of the existing particle flux models (MASTER and ORDEM) to allow for more reliable impact risk assessments in the future.

### Calibration of Results

To convert from crater sizes (obtained from the images) to particle sizes (output from the flux models), so called damage equations are required. For the outer surface of Columbus such equations are available at least for similar Aluminum alloys in generic set-ups. The applicability of available damage equations for the Columbus MDPS shall be assessed during the analysis phase.

In case the applicability needs to be verified, hypervelocity impact experiments can be performed for relevant particle sizes on nominal identical surface material. Besides verification of the damage equations for the Columbus MDPS material, experiments provide the possibility to obtain the impact conditions for observed non-standard impact features. Information of existing impact tests on the Columbus MDPS are not useful for this purpose, since the impacts performed before the flight of Columbus were at the upper end of the MDPS capabilities, i.e. to proof the low probability of a harmful impact on the Columbus module.

### Utilization of Results

The output from the image processing will be further analyzed (counted and sorted by size) and compared to the MASTER population. The Columbus mission will be the longest in-orbit evaluated surface due to its 10 year mission and would represent the most recent impact data since it covers the years 2008 to 2018. Therefore, it represents a very valuable data source for the calibration

and validation of ESA's MASTER and other space debris and meteoroid models. Especially the observable diameter spectrum currently has very limited data available which makes the Columbus impact survey a very important data source.

The generation of the MASTER population is done on a regular basis in order to provide the space community with the most recent and updated model on the space debris environment. Impact data from the Columbus mission will be permanently integrated in the validation cycle, ensuring an accurate model for the space debris environment provided by ESA's MASTER. Same as for all currently available validation data, the Columbus impact data will be compared with the MASTER model to identify shortcomings and modelling drawbacks. Whereas the agreement between MASTER and the currently available validation data is sufficiently accurate, there is no information on the small objects population for this decade, more precisely after 2002. Having the Columbus impact data available, which provides data from 2008 up to today, directly supports all tools that rely on the MASTER population.

#### Measurement Method

It should be noted that the measurement method is a unique opportunity, since the surveyed surface ("sensor surface") neither features any possibilities for an active impact recording nor is it retrieved to Earth and investigated in a laboratory. Instead, the unique imaging capabilities available onboard the ISS are utilized to convert a passive, inactive surface to a sensor surface.

#### CONCLUSIONS & OUTLOOK

A survey of a large ISS module, like Columbus, offers a unique opportunity to gain valuable new information on the abundant population of meteoroids and debris in space.

After 10 years in orbit in an altitude between 335 and 420 km, the outside shell of the Columbus module offers an unprecedented source of information on space debris and micrometeoroid impacts in space. Hundreds of impact craters larger than 1 mm are expected. The forward side of Columbus was nearly all the time facing in flight direction, giving a reliable basis for comparison of the number of impacts with model predictions.

The present survey (utilization of the robotic arm and related camera equipment for the survey) could be complemented by a second survey during an EVA or using a higher resolution camera from VIPIR2, covering a part of the robotic survey a second time as reference with a different equipment and higher resolution.

For such high detector resolutions, the three-dimensional morphology of the surface and hence the impact craters could potentially be reconstructed [27]. The crater shape would enable us to infer on the density of the impactor and the impact direction, thus

complementing our understanding of individual impact processes.

The results of this survey will be compared to numerical model predictions and if required the models will be improved leading to more reliable impact risk assessments for future missions.

#### ACKNOWLEDGEMENTS

We would like to acknowledge the great support that this survey has received so far in a great number of ways: Berti Meisinger, ESA Columbus Mission Director, has supported us greatly and finally managed to put the survey onto the schedule together with Jan Marius Bach, DLR Columbus Lead Flight Director. Julia Weis succeeded Berti Meisinger as ESA Columbus Mission Director and supported us to conclude the survey. Daniele Laurini from ESA's Human and Robotics Exploration Section helped to make the activity possible. The NASA Robotics Operations Branch conducted the survey: Kenton Kirkpatrick supported us greatly in defining the best implementation for the survey and in coordination; section A of the survey was performed by Heidi Jennings, Jason Seagram, Cash Donahoe, Billy Jones and Tyler Minish; section B of the survey was performed by Jared Olson, Frank Jurgens, Brandy Holmes, Melanie Miller, Danielle Cormier and Jayanta Ray; and Chris Andrew was the increment lead who made the scheduling of the operation happen. The NASA Image Science and Analysis Group – Michael Rollins and Gary Kilgo – supported us with background information and sample video data to plan the survey. Todd W. Hellner, Julie A. Dunning and T. J. Creamer, all NASA, also supported the survey. We are aware that with any operation onboard the ISS a great number of people are involved directly and indirectly. We named all those whom we had direct contact to during the survey, but would also like to express our gratitude to those who supported the activity in the background. Finally, we would like to thank anybody who keeps or kept running the ISS in general and specifically the Columbus module, and without whom the survey would also not have been possible.

#### REFERENCES

- [1] SPACE RESEARCH TODAY: ESA declares end of mission for Envisat. In: *Space Research Today* 184 (2012), pp. 13-14. – <https://doi.org/10.1016/j.srt.2012.07.012>
- [2] MERHOLZ, D.; LEUSHACKE, L.; FLURY, W.; JEHN, R.; KLINKRAD, H.; LANDGRAF, M.: Detecting, tracking and imaging space debris. In: *esa bulletin* 109 (2002), pp. 128-134
- [3] JOHNSON, N. L.; STANSBERRY, E.; WHITLOCK, D. O.; ABERCROMBY, K. J.; SHOOT, D.: *History of On-Orbit Satellite Fragmentations, 14th Edition*. Houston, TX, USA : NASA, 2008. – NASA/TM-2008-214779



- [4] SÁNCHEZ-ORTIZ, N.; DOMÍNGUEZ-GONZÁLEZ, R.; KRAG, H.; FLOHRER, T.: Impact on mission design due to collision avoidance operations based on TLE or CSM information. In: *Acta Astronautica* 116 (2015), No. Supplement C, pp. 368-381. – <https://doi.org/10.1016/j.actaastro.2015.04.017>
- [5] NATIONAL RESEARCH COUNCIL: *Limiting future collision risk to spacecraft: an assessment of NASA's meteoroid and orbital debris programs*. Washington, D.C. : The National Academies Press, 2011. – ISBN 978-9-309-21974-4
- [6] KEMPF, S., et al.: Risk and vulnerability analysis of satellites due to MM/SD with PIRAT. In: OUWEHAND, L. (Ed.); *Proc. 6th European Conference on Space Debris*. ESOC, Darmstadt, Germany, 2013. – ESA SP-723
- [7] KRISKO, P. H.; FLEGEL, S.; MATNEY, M. J.; JARKEY, D. R.; BRAUN, V.: ORDEM 3.0 and MASTER-2009 modeled debris population comparison In: *Acta Astronautica* 113 (2015), pp. 204-211. – <https://doi.org/10.1016/j.actaastro.2015.03.024>
- [8] BAUER, W.; ROMBERG, O.; PUTZAR, R.: Experimental verification of an innovative debris detector. In: *Acta Astronautica* 117 (2015), pp. 49-54. – <https://doi.org/10.1016/j.actaastro.2015.07.008>
- [9] SPENCER, G. T.; SCHÄFER, F. K.; TANAKA, M.; WEBER, M.; PUTZAR, R.; JANOVSKY, R.; KALNINS, I.: Design and initial calibration of micrometeoroid/space debris detector (MDD). In: DANESY, D. (Ed.); *Proc. 4th European Conference on Space Debris*. Darmstadt, Germany, 2005, pp. 227-232. – ESA SP-587
- [10] DROLSHAGEN, G.; McDONNELL, T.; MANDEVILLE, J.-C.; MOUSSI, A.: Impact studies of the HST solar arrays retrieved in March 2002. In: *Acta Astronautica* 58 (2006), No. 9, pp. 471-477. – <https://doi.org/10.1016/j.actaastro.2005.12.011>
- [11] BERNHARD, R. P.; CHRISTIANSEN, E. L.; HYDE, J.; CREWS, J. L.: Hypervelocity impact damage into space shuttle surfaces. In: *International Journal of Impact Engineering* 17 (1995), No. 1, pp. 57-68. – [https://doi.org/10.1016/0734-743X\(95\)99835-F](https://doi.org/10.1016/0734-743X(95)99835-F)
- [12] FLEGEL, S., et al.: *Maintenance of the ESA MASTER model*. Braunschweig : TU Braunschweig, Institute of Aerospace Systems, 2011. – RFQ No 21705/08/D/HK
- [13] FIEDLER, H.; HERZOG, J.; PROHASKA, M.; SCHILDKNECHT, T.; WEIGEL, M.: SMARTnet - status and statistics. In: *Proc. 68th International Astronautical Congress*. Adelaide, Australia, 2017. – IAC-17-A6.1.2
- [14] LAMBERT, M.; SCHÄFER, F.; GEYER, T.: Impact damage on sandwich panels and multi-layer insulation. In: *International Journal of Impact Engineering* 26 (2001), pp. 369-380. – [https://doi.org/10.1016/S0734-743X\(01\)00108-7](https://doi.org/10.1016/S0734-743X(01)00108-7)
- [15] SCHNEIDER, E. E.; SCHÄFER, F. K.; DESTEFANIS, R.; LAMBERT, M.: Advanced shields for manned space modules. In: *Proc. 55th International Astronautical Congress*. Vancouver, Canada, 2004. – IAC-04-IAA.5.12.2.01
- [16] KRAG, H., et al.: A 1 cm space debris impact onto the Sentinel-1A solar array. In: *Acta Astronautica* 137 (2017), pp. 434-443. – <https://doi.org/10.1016/j.actaastro.2017.05.010>
- [17] BRUMFIEL, G.; KWOK, R.: Kaputnik chaos could kill Hubble. In: *Nature* 457 (2009), No. 7232, pp. 940-941. – <https://doi.org/10.1038/457940a>
- [18] SPACEDAILY: *Russian telecom satellite fails after sudden impact*. URL [http://www.spacedaily.com/reports/Russian\\_Telecom\\_Satellite\\_Fails\\_After\\_Sudden\\_Impact.html](http://www.spacedaily.com/reports/Russian_Telecom_Satellite_Fails_After_Sudden_Impact.html). – access: 2006-03-30
- [19] WIEDEMANN, C.; DIETZE, C.; STABROTH, S.; FLEGEL, S.; ALWES, D.; VÖRSMANN, P.: Damage cost of space debris impacts on historical satellites. In: *Proc. 59th International Astronautical Congress*. Glasgow, Scotland, UK, 2008. – IAC-08-A6.2.10
- [20] McDONNELL, J. A. M.; UNISPACE KENT; ONERA; NATIONAL HISTORY MUSEUM: *Post-Flight Impact Analysis of HST Solar Arrays - 2002 Retrieval, Contract No. 16283/NL/LvH, Final Report*, 2005
- [21] NASA: *Columbus module image from STS-127 crew* : Wikipedia, 2009. – URL [https://de.wikipedia.org/wiki/Datei:Columbus\\_module\\_-\\_cropped.jpg](https://de.wikipedia.org/wiki/Datei:Columbus_module_-_cropped.jpg). – image ID s127e009781
- [22] NASA: *Orbital debris education package*. Houston, Texas : NASA Johnson Space Center, 2004. – <https://de.scribd.com/document/39269482/Orbital-Debris-Education-Package>
- [23] ROLLINS, M.; MOORE, R.; KILGO, G.: Soyuz inspection. In: *Proc. 3rd In-Space Inspection Workshop 2017*. NASA Johnson Space Center, Houston, 2017. – JSC-CN-38484
- [24] FLEGEL, S., et al.: *MASTER-2009 software user manual*. Braunschweig : TU Braunschweig, Institute of Aerospace Systems, 2011. – RFQ No 21705/08/D/HK
- [25] RUDOLPH, M.; SCHÄFER, F.; DESTEFANIS, R.; FARAUD, M.; LAMBERT, M.: Fragmentation of hypervelocity aluminum projectiles on fabrics. In: *Acta Astronautica* 76 (2012), pp. 42-50. – <https://doi.org/10.1016/j.actaastro.2012.02.002>
- [26] OTSU, N.: A threshold selection method from gray-level histograms. In: *IEEE Transactions on Systems, Man, and Cybernetics* 9 (1979), No. 1, pp. 62-66. – <https://doi.org/10.1109/TSMC.1979.4310076>
- [27] GULDE, M.; BERGER, H.; PUTZAR, R.: Stereoscopic imaging determines space debris impact crater distribution and morphology In: *Aeronautics and Aerospace Open Access Journal* 1 (2017), No. 4, p. 00021. – <https://doi.org/10.15406/aaaj.2017.01.00021>